IEEE Access
Multidisciplinary ⋮ Rapid Review ⋮ Open Access Journal

Received December 26, 2020, accepted January 21, 2021, date of publication February 4, 2021, date of current version March 1, 2021.

Digital Object Identifier 10.1109/ACCESS.2021.3056542

Closed-Form Representations of Friction

JIN HUANG, XINGYU LI, HUIQIAN LI, YE-HWA CHEN, AND ZHIHUA ZHONG
School of Vehicle and Mobility, Tsinghua University, Beijing 100084, China

Corresponding author: Ye-Hwa Chen (yehwa.chen@me.gatech.edu)

This work was supported in part by the NSFC Program under Grant 61872217, Grant U20A20285, Grant U1701262, and Grant U1801263; and in part by the Industrial Internet Innovation and Development Project of Ministry of Industry and Information Technology.

ABSTRACT The current developed friction models are basically based on the assumption of the normal forces exerted between the contact surfaces known in advance, less work has been done for closed-form (i.e., analytic) modeling in complex mechanical systems where the normal forces vary greatly over time. In this paper, the closed-form representations of friction forces in mechanical systems are newly derived in a way of dynamics. The Udwadia-Kalaba equation is first used to calculate the normal force exerted by the contact surface in mechanical system. The friction force is then calculated via existing friction models. Such closed-form expressions of friction forces contain both the magnitude and direction at any instant of time, even as the normal force is nonconstant. The novel representations offer an effective way for analytically expressing friction force in dynamical systems, which makes it possible for accurate simulation and control design of dynamical systems with non-negligible friction forces.

INDEX TERMS Friction force, closed-form modeling, mechanical systems, robotics.

I. INTRODUCTION

Friction was studied extensively in classical mechanical engineering and there has lately been a strong resurgence driven by strong engineering needs in a wide range of industries, especially for the control engineering. Friction is highly nonlinear and may result in steady state errors, limit cycles, and poor performance in control engineering [1]. To eliminate the control and simulation errors caused by friction force in dynamical systems, explicit closed-form representations of friction force in mechanical system are deeply required.

The dominant friction phenomena that have been modeled generally include stiction, Coulomb friction, viscous friction, Stribeck effect, asymmetries and position dependence etc. Different friction models may capture different friction phenomena. Rather than the classical friction models (i.e., the Coulomb friction model and the stiction model), much effort has been put on developing the extended friction models in mechanical systems for control engineering. Plenty of friction models were developed based on experiments and mathematical derivations [2]–[9], include the well-known Dahl model, LuGre model, Leuven model and the Generalized Maxwell Slip model, etc. Friction models are generally classified into two groups, the static friction models and the dynamic friction models. New research on developing friction models is still ongoing, which either focuses on the effectiveness or governing more friction effects, see e.g., [10]–[12]. There are also many researches on parameter identification and model improvement. It is shown that most of the current known friction models (static or dynamic) are based on the knowledge of normal forces exerted between the contact surfaces. Reference [13] offered one representation of friction for planar objects, which models the reaction forces generated by a point of contact. However, when it is generalized to three-dimensional rigid bodies, difficulties arise.

Although much effort has been done on obtaining the friction models for mechanical systems, nearly all of the work is approximate in nature, that is, they consider the normal forces exerted between the contact surfaces being known in advance. This leads the applications of such friction models hardly to avoid using constant normal forces, which happened even in some nonlinear mechanical systems (see, e.g., [14], [15]). What is more, the absence of the closed-form friction models in control design area costs much effort on the research of either model-based or non-model-based friction compensation [16]–[21], sensor-based or nonsensor-based normal forces evaluation/prediction [22]–[24] and some ingenious solutions through numerical approaches [25]–[27]. We stress that the processes of the above researches are rather successful. Nevertheless, analytical friction models

The associate editor coordinating the review of this manuscript and approving it for publication was Yangmin Li.

may simplify such work for accurate system simulation and control design.

Literature reviews showed that little work has been done on closed-form friction force modeling for complex (i.e., non-block-simple) mechanical systems where the normal forces being nonconstant. The current literature, takes closed-form friction force modeling problems in a quite different view, i.e., from the view of dynamics, and thus makes it possible to model closed-form friction forces for any constrained mechanical system. We take the proposed approach as an adequate supplement to the current known friction models. By friendly combination with the current known friction models, the literature succeeds to provide the closed-form expressions of friction force in constrained mechanical systems. The closed-form expressions are given not only for the classic friction models, but also for the extended friction models. Such closed-form expressions can be used for system design and simulation wherever there is non-negligible friction force presented in a mechanical system, no matter whether the normal force exerted between the contact surfaces is constant or not. With the adequate supplement to the current known friction models, the literature may propose a new way for doing accurate friction modeling and applications.

II. THE UDWADIA-KALABA EQUATION

Consider a discrete mechanical system whose configuration is described by the coordinate $q = \begin{bmatrix} q_1 & q_2 & \cdots & q_n \end{bmatrix}^T \in \boldsymbol{R}^n$, thus the generalized velocity $\dot{q} = \begin{bmatrix} \dot{q}_1 & \dot{q}_2 & \cdots & \dot{q}_n \end{bmatrix}^T \in \boldsymbol{R}^n$, and the generalized acceleration $\ddot{q} = \begin{bmatrix} \ddot{q}_1 & \ddot{q}_2 & \cdots & \ddot{q}_n \end{bmatrix}^T \in \boldsymbol{R}^n$. Suppose the system is under a resultant external force $Q(\dot{q}, q, t)$. we have

$$M(q,t)\ddot{q} = Q(\dot{q}, q, t), \tag{1}$$

where $M(q,t) = M^T(q,t) \in \boldsymbol{R}^{n\times n} > 0$ is the mass matrix.

The above system without imposing any additional constraints is called an *unconstrained system* [28]. Now suppose the unconstrained system is subjected to a set of constraints in the matrix form of

$$A(q,t)\dot{q} = c(q,t). \tag{2}$$

In addition, the virtual displacement $\delta q \in \boldsymbol{R}^n$, which lies in the null space formed by $A(q,t)$, is governed by

$$A(q,t)\delta q = 0. \tag{3}$$

The presence of the constraints in (2) will apply additional constraint force Q^c, so the equation of motion of the constrained system is then

$$M(q,t)\ddot{q} = Q(\dot{q}, q, t) + Q^c, \tag{4}$$

The constraint force Q^c is to be determined, which is one of the main objectives in constrained mechanical system modeling.

Remark 1: The constraints in (2), in general, can either be ideal or nonideal. Ideal constraints will generate ideal constraint forces (all the forces that subject to D'Alembert's Principle), and nonideal constraints will generate nonideal constraint forces (forces that defy D'Alembert's Principle, e.g., friction force, electro-magnetic force, etc.). Thus, if there are both ideal and nonideal constraints present in the system, we will have

$$Q^c = Q^c_{id} + Q^c_{nid} \tag{5}$$

where Q^c_{id} is the ideal constraint force and Q^c_{nid} is the nonideal constraint force.

Reference [29] extended the D'Alembert's Principle to include nonideal constraints. For any virtual displacement δq subjected to (3), the total work W done by the constraint forces due to nonideal constraints at each instant of time t is such that $W = \delta q^T C$, where $C(q, \dot{q}, t) \in \boldsymbol{R}^n$ is a known vector that may be determined for the specific dynamical system under consideration through experimentation, analogous with other systems, or otherwise.

Taking the time derivative of the (first order) constraint (2), we have the following second order form

$$A(q,t)\ddot{q} = b(\dot{q}, q, t), \tag{6}$$

where

$$b(\dot{q}, q, t) := \dot{c}(\dot{q}, q, t) - \left(\frac{\mathrm{d}}{\mathrm{d}t}A(\dot{q}, q, t)\right)\dot{q}. \tag{7}$$

It has been shown that [29]

$$\begin{aligned} Q^c_{id}(\dot{q}, q, t) &= M^{\frac{1}{2}}(q,t)B^{+}(q,t)(b(\dot{q}, q, t) - A(q,t) \\ &\quad \times M^{-1}(q,t)Q(\dot{q}, q, t)), \end{aligned} \tag{8}$$

$$\begin{aligned} {}^{c}_{nid}(\dot{q}, q, t) &= M^{\frac{1}{2}}(q,t)(I - B^{+}(q,t)B(q,t)) \\ &\quad \times M^{-\frac{1}{2}}(q,t)C(\dot{q}, q, t), \end{aligned} \tag{9}$$

where $B(q,t) := A(q,t)M^{-\frac{1}{2}}(q,t)$ and "+" denotes the generalized Moore-Penrose inverse. Thus the closed-form expression of the equation of motion that governs the evolution of the constrained system is

$$\begin{aligned} M(q,t)\ddot{q} = {} & Q(\dot{q}, q, t) + M^{\frac{1}{2}}(q,t)B^{+}(q,t) \\ & \times (b(\dot{q}, q, t) - A(q,t)M^{-1}(q,t)Q(\dot{q}, q, t)) \\ & + M^{\frac{1}{2}}(q,t)(I - B^{+}(q,t)B(q,t)) \\ & \times M^{-\frac{1}{2}}(q,t)C(\dot{q}, q, t). \end{aligned} \tag{10}$$

This is the *Udwadia-Kalaba equation* for the system that is subject to both ideal and nonideal constraints.

Remark 2: The constraint forces in (8) and (9) are shown in closed-form, without referring to the Lagrange multiplier. In addition, the Udwadia-Kalaba equation is applicable to all holonomically and non-holonomically constraints.

Remark 3: Equation (9) shows the closed-form expression of Q^c_{nid} based on $C(\dot{q}, q, t)$. However, the vector $C(\dot{q}, q, t)$ is case-dependent and may need additional effort to obtain. In addition, besides friction force, the nonideal constraint force may include other forms of force. Therefore, Q^c_{nid} in (9) may not serve the purpose of expressing the friction force. We may need to take a deeper look at the force distribution on the constraint surface.

III. THE FORCE DIAGRAM

For the mechanical system (10), the constraint surface is governed by (2). At time t, assume the contact point with the constraint surface is O (Figure 1). It moves at a generalized velocity $\dot{q}(t)$, which is the actual velocity, among all possible velocity. The actual velocity $\dot{q}(t)$ is tangent to the constraint surface.

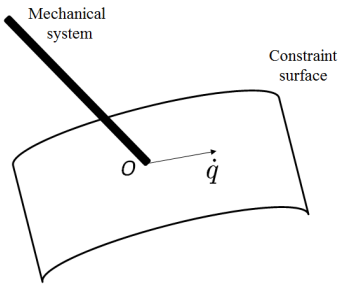

FIGURE 1. Mechanical system and the constraint surface.

Assume $rank(A) \geq 1$. Q can be decomposed into two orthogonal components suggest that ([30], see the theorem in Appendix A)

$$Q(\dot{q}, q, t) = Q_p(\dot{q}, q, t) + Q_t(\dot{q}, q, t), \tag{11}$$

where

$$Q_p(\dot{q}, q, t) := A^+(q, t)A(q, t)Q(\dot{q}, q, t), \tag{12}$$
$$Q_t(\dot{q}, q, t) := (I - A^+(q, t)A(q, t))Q(\dot{q}, q, t). \tag{13}$$

Here $Q_p \in \mathcal{R}(A^T)$ is perpendicular to the constraint surface and $Q_t \in \mathcal{N}(A)$ is tangent to the constraint surface.

At an instant time t, the force diagram is shown in Figure 2. The ideal constraint force Q^c_{id}, which lies in the range space of A^T, does no work under virtual displacement and thus is perpendicular to the constraint surface (as well as $\dot{q}$). This is the *normal force* at the constraint surface. The nonideal constraint force Q^c_{nid}, which does work under virtual displacement, is tangent to the constraint surface but may deflect a certain angle from $\dot{q}(t)$. Thus $Q^c_{id} + Q_p$ will be the resultant force that is perpendicular to the constraint surface, and $Q^c_{nid} + Q_t$ will be the resultant force that is tangent to the constraint surface. Note that the two resultant forces work on supplying the accelerations both perpendicular and tangent to the constraint surface.

Remark 4: When in the special case that $\dot{q} \equiv 0$ (i.e., $\dot{q} = 0$ and $\ddot{q} = 0$), we have

$$Q^c_{id} + Q_p \equiv 0, \quad Q^c_{nid} + Q_t \equiv 0. \tag{14}$$

The constraint forces, both ideal and nonideal, are generated to prevent the system from moving. Specifically, Q_t is the force that makes the system to tend to move along a direction tangent to the constraint surface and Q^c_{nid} is generated to compensate Q_t. If there is only friction force present as nonideal constraint force in the system, this is right the situation when *stiction* occurs. In addition, Q^c_{id} is the "contact" force (i.e., normal force) between the constraint surfaces and the system at the constraint point. With the force diagram analyzed in this section, we start to work on friction force next.

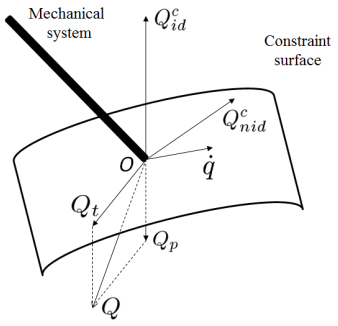

FIGURE 2. Force diagram at the constraint.

IV. THE CLOSED-FORM FRICTION FORCE: COULOMB FRICTION AND STICTION

If there is friction force present in the constraint mechanical system at the constraint point, the friction force will be part of, or equal to, Q^c_{nid}. In this paper, we assume there is only friction force present as nonideal constraint force in the system.

The force diagram in last section is with n-dimensional, the friction force in mechanical system, in general, occurs in maximum three dimensional world. Thus we may need a *Jacobian matrix* for transforming use. Define a vector $p(t) = \left[x(t)\ y(t)\ z(t)\right]^T$, $p(t) \in \boldsymbol{R}^3$ as the coordinate of the constraint point in *Cartesian system*. Assume we have the kinematic relations $x = f_x(q, t)$, $y = f_y(q, t)$, $z = f_z(q, t)$. The Jacobian matrix is then given by

$$J(q, t) := \begin{bmatrix} \frac{\partial f_x(q,t)}{\partial q_1} & \frac{\partial f_x(q,t)}{\partial q_2} & \cdots & \frac{\partial f_x(q,t)}{\partial q_n} \\ \frac{\partial f_y(q,t)}{\partial q_1} & \frac{\partial f_y(q,t)}{\partial q_2} & \cdots & \frac{\partial f_y(q,t)}{\partial q_n} \\ \frac{\partial f_z(q,t)}{\partial q_1} & \frac{\partial f_z(q,t)}{\partial q_2} & \cdots & \frac{\partial f_z(q,t)}{\partial q_n} \end{bmatrix}. \tag{15}$$

Here $J(q, t) \in \boldsymbol{R}^{3\times n}$. We assume that $J(q, t)$ has full rank (i.e., $rank(J(q, t)) = 3$). Denote Q_ϵ the *generalized force* and F_ϵ the corresponding *Cartesian force*, using the Jacobian matrix, we will have the following relations

$$\dot{p}(t) = J(q(t), t)\dot{q}(t), \tag{16}$$
$$Q_\epsilon(t) = J^T(q(t), t)F_\epsilon(t), \tag{17}$$
$$F_\epsilon(t) = (J(q(t), t)J^T(q(t), t))^{-1}J(q(t), t)Q_\epsilon(t). \tag{18}$$

Remark 5: For the spatial problem, the constraint point is orientated by the Cartesian coordinate p in Cartesian system, or equivalently orientated by the generalized coordinate q in generalized n-dimensional space. For most mechanical systems, we have $n \geq 3$. Thus the assumption that the Jacobian matrix $J(q)$ is of full rank 3 can be easily achieved.

Denote F_n as the normal force at the constraint point in Cartesian system, F_t as the tangential force at the constraint point in Cartesian system corresponding to Q_t. From (8), (13)

and (18), we have

$$\begin{aligned} F_n(t) &:= (J(q(t),t)J^T(q(t),t))^{-1}J(q(t),t)Q_{id}^c(\dot{q}(t),q(t),t) \\ &= (J(q(t),t)J^T(q(t),t))^{-1}J(q(t),t) \\ &\quad \times M^{\frac{1}{2}}(q(t),t)B^+(q(t),t)(b(\dot{q}(t),q(t),t) \\ &\quad -A(q(t),t)M^{-1}(q(t),t)Q(\dot{q}(t),q(t),t)), \qquad (19) \\ F_t(t) &:= (J(q(t),t)J^T(q(t),t))^{-1}J(q(t),t)Q_t(\dot{q}(t),q(t),t) \\ &= (J(q(t),t)J^T(q(t),t))^{-1}J(q(t),t) \\ &\quad \times (I-A^+(q(t),t)A(q(t),t))Q(\dot{q}(t),q(t),t). \qquad (20) \end{aligned}$$

Knowing that F_n and F_t are explicitly given in closed-form, the closed-form of *Coulomb friction* and *Stiction* can be derived.

A. *Coulomb Friction*. The Coulomb friction model describes the kinetic friction force where there is relative motion at contact. The closed-form expression of Coulomb friction F_c in Cartesian system can be given as

$$F_c(t) = -\mu\|F_n(t)\|\hat{p}(t), \quad \hat{p} \neq 0, \qquad (21)$$

where μ is the *coefficient of friction*, F_n is from (19), and

$$\hat{p}(t) := \dot{p}(t)/\|\dot{p}(t)\|, \quad \dot{p} \neq 0 \qquad (22)$$

is an unit vector representing the motion direction. Using (16), we have

$$\hat{p}(t) = J(q(t),t)\dot{q}(t)/\|J(q(t),t)\dot{q}(t)\|, \quad \dot{q} \neq 0. \qquad (23)$$

Throughout the paper, $\|\cdot\|$ denotes the Euclidean norm.

By (17), the closed-form *generalized Coulomb friction force* expressed in the generalized coordinates will be

$$Q_c(\dot{q},q,t) := -\mu J^T(q,t)\|F_n(t)\|\frac{J(q,t)\dot{q}}{\|J(q,t)\dot{q}\|}, \quad \dot{q} \neq 0. \qquad (24)$$

B. *Stiction*. Stiction model is to describe the static friction, which must be overcome by an applied force before an object can move. From the instant sliding occurs, static friction is no longer applicable. Denote F_m as the maximum possible stiction in Cartesian system, the magnitude of F_m will be

$$\|F_m(t)\| = \mu_s\|F_n(t)\| \qquad (25)$$

where μ_s be the *coefficient of static friction*, F_n is again from (19). Note that F_m is time variant since F_n is time variant. Knowing that F_t in (20) is the tangential force, the closed-form expression of the stiction in Cartesian system, denoted as F_s, is case-wisely,

$$F_s(t) = \begin{cases} -F_t(t), & \dot{q} = 0 \ \& \ \|F_t\| \leq \|F_s\| \\ -\mu_s\|F_n(t)\|\hat{f}(t), & \dot{q} = 0 \ \& \ \|F_t\| > \|F_s\|. \end{cases} \qquad (26)$$

where $\hat{f} := F_t(t)/\|F_t(t)\|$ is also an unit vector. With (13), similar with (24), the *generalized stiction* expressed in the generalized coordinates will be

$$Q_s(t) = \begin{cases} -Q_t, & \dot{q} = 0 \ \& \ \|F_t\| \leq \|F_s\| \\ -\mu_s J^T(q,t)\|F_n(t)\|\hat{f}(t), & \dot{q} = 0 \ \& \ \|F_t\| > \|F_s\|. \end{cases} \qquad (27)$$

Remark 6: One may want to combine (24) and (27) together to express both the Coulomb friction and the static friction. Using Q_f to denote the generalized friction force, we then have the closed-form

$$Q_f = \begin{cases} -\mu J^T\|F_n\|\hat{p}, & \dot{q} \neq 0 \\ -Q_t, & \dot{q} = 0 \ \& \ \|F_t\| \leq \|F_s\| \\ -\mu_s J^T\|F_n\|\hat{f}, & \dot{q} = 0 \ \& \ \|F_t\| > \|F_s\|, \end{cases} \qquad (28)$$

with F_n from (19).

Remark 7: Equations (24), (27) and (28) are closed-form expressions of friction force for spatial systems. For a planar system, the coordinates is then $p = [x, \ y]^T$, the Jacobian matrix in (15) is then become

$$J(q,t) = \begin{bmatrix} \frac{\partial f_x(q,t)}{\partial q_1} & \frac{\partial f_x(q,t)}{\partial q_2} & \cdots & \frac{\partial f_x(q,t)}{\partial q_n} \\ \frac{\partial f_y(q,t)}{\partial q_1} & \frac{\partial f_y(q,t)}{\partial q_2} & \cdots & \frac{\partial f_y(q,t)}{\partial q_n} \end{bmatrix}, \qquad (29)$$

the closed-form expressions of friction forces are still held.

Remark 8: In the special scalar case, we have $J \equiv 1$. Thus we have $F_n = Q_{id}^c = Q_p$, $F_t = Q_t$. Define a sign function

$$sgn(\alpha) := \begin{cases} -1, & \alpha < 0 \\ 0, & \alpha = 0 \\ 1, & \alpha > 0. \end{cases} \qquad (30)$$

Let v be the scalar velocity of the system motion, equation (28) is then

$$Q_f = \begin{cases} -\mu\|F_n\|sgn(v), & v \neq 0 \\ -F_t, & v = 0 \ \& \ \|F_t\| \leq \|F_s\| \\ -\mu_s\|F_n\|sgn(F_t), & v = 0 \ \& \ \|F_t\| > \|F_s\|, \end{cases} \qquad (31)$$

thus the classic scalar form introduced in most textbooks.

Remark 9: With using the newly developed closed-form normal force representations, we have the closed-form representations of the classic friction models. We would expect that it will not change the behaviors of the classic friction models for some practical conditions (e.g., shape of the contact surfaces, elastic or inelastic collision, slip behavior of the elastic surface, etc.). However, this is out of the scope of the current paper and may be studied elsewhere for further verification through certain experiments.

V. THE CLOSED-FORM FRICTION FORCE: EXTENDED FRICTION MODELS

Plenty of extended friction models, which are more accurate in presenting the friction phenomena, are developed, e.g., the Dahl model, the LuGre model, etc. as referenced in the Introduction. Most of the extended models are, interestingly, dependent on the magnitude of the Coulomb friction, say $\|F_c\|$, and/or the magnitude of maximum possible stiction, say $\|F_m\|$. However, Nearly all the current known models are approximate in nature as they suffer from using a constant exerted normal force.

From (21), the magnitude of the Coulomb friction is $\|F_c\| = \mu\|F_n\|$ and the magnitude of the maximum stiction

is given in (25). With (19), we have

$$\|F_c\| = \mu \left\| (JJ^T)^{-1} J M^{\frac{1}{2}} B^{+} (b - AM^{-1}Q) \right\|, \quad (32)$$

$$\|F_m\| = \mu_s \left\| (JJ^T)^{-1} J M^{\frac{1}{2}} B^{+} (b - AM^{-1}Q) \right\|. \quad (33)$$

Having the closed form expressions of both $\|F_c\|$ and $\|F_m\|$, it is thus possible to give the closed-form expressions of the extended friction models. We illustrate the idea by giving the explicit expressions of the Dahl model.

The Dahl model introduced in [2] was developed for the purpose of simulating control systems. Starting from stress-strain curve in classical solid mechanics, Dahl modeled the stress-strain curve by a differential equation. The model is given in the scalar form. Let F_d be the friction force of Dahl model, then the model takes the form of

$$\frac{\mathrm{d}F_d}{\mathrm{d}s} = \sigma \left(1 - \frac{F_d}{\|F_c\|} sgn(v)\right)^{\alpha}, \quad (34)$$

where s is the displacement, v is the relative velocity, σ is the stiffness coefficient and α is a parameter that determines the shape of the stress-strain curve, $\|F_c\|$ is the magnitude of F_c but in the scalar case. F_d can then be calculated by a time domain Dahl model of

$$\frac{\mathrm{d}F_d}{\mathrm{d}t} = \frac{\mathrm{d}F_d}{\mathrm{d}s}\frac{\mathrm{d}s}{\mathrm{d}t} = \sigma \left(1 - \frac{F_d}{\|F_c\|} sgn(v)\right)^{\alpha} v. \quad (35)$$

The Dahl model is a generalization of ordinary Coulomb friction and it does not capture stiction, so it is only applicable to the case when $v \neq 0$.

We generalize the above parameters into a spatial case. Denote x, y, z as the displacements along the axis of the Cartesian system (generalization of s), thus $\dot{x}, \dot{y}, \dot{z}$ as the corresponding velocity (generalization of v). Similarly, denote $\sigma_x, \sigma_y, \sigma_z$ as the stiffness coefficient along x, y, z, $\alpha_x, \alpha_y, \alpha_z$ as the shape parameters along x, y, z, F_{cx}, F_{cy}, F_{cz} as the Coulomb friction along x, y, z, and F_{dx}, F_{dy}, F_{dz} as the corresponding Dahl friction force. Thus the generalized Dahl model for spatial system is, for $k = x, y, z$ and $\dot{k} \neq 0$,

$$\frac{\mathrm{d}F_{dk}}{\mathrm{d}t} = \sigma_k \left(1 - \frac{F_{dk}}{\|F_{ck}\|} sgn(\dot{k})\right)^{\alpha_k} \dot{k}. \quad (36)$$

Here $\|F_{ck}\|$, the norm of Coulomb friction along each direction, can be calculated by using (32). No matter whether the normal force is constant or not, we have $\|F_{ck}\| = \|F_c\| \frac{\|\dot{k}\|}{\|\dot{p}\|}$ $\dot{k} \neq 0$. Here the vector p is from the vector defined above (15). F_{dx}, F_{dy}, F_{dz} in (36) can then be explicitly solved. Thus the Dahl friction force for the spatial system in Cartesian system is $F_d = [-F_{dx} \ -F_{dy} \ -F_{dz}]^T$, and the generalized Dahl friction force is then $Q_d = J^T F_d$.

Remark 10: The Dahl model is initially developed only for one dimensional problems. We generalize the model to be applicable to the spatial case and each direction is taken equally as an one dimensional problem. The resultant friction force is then gathered from all three dimensions. Other extended models related with F_c and F_m (or maybe with F_t as well) can follow the same way and will no more suffer from the assumption of the applied normal force be constant.

Remark 11: Different extended friction models may capture different friction phenomena. Since most of the extended friction models are developed to model the dynamic phenomenon (e.g., stick-slip friction, oscillation, viscous friction, Stribeck effect, etc.), the proposed closed-form representation of friction force will inherit the properties of the employed friction model. Readers shall choose proper friction model for capturing different friction phenomena.

VI. ILLUSTRATIVE EXAMPLES

We first employ the simple horizontal sliding block system in Figure 3 for validating the proposed modeling approach. Assume the mass of the block is m, then the gravity force is $-mg$ with g be the gravitational acceleration. An external force F acts on the block and there is friction force f between the block and floor. The coefficient of friction is μ. We thus simply know that for Coulomb friction model, the normal force $F_n = mg$, and the friction force $f = -\mu mg$ according to the given coordinates in Figure 3.

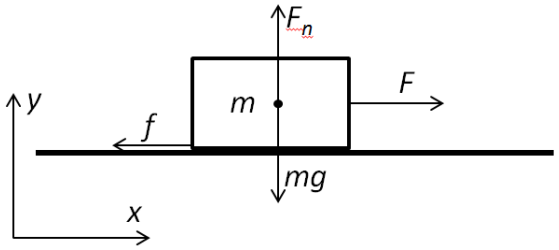

FIGURE 3. Horizontal sliding block system.

To validate the effectiveness of the proposed approach, we model the normal force F_n and the friction force f by the proposed approach. We have the system equation as:

$$M\ddot{q} = Q + F_n + f, \quad (37)$$

where

$$M = \begin{bmatrix} m & 0 \\ 0 & m \end{bmatrix}, \quad q = \begin{bmatrix} x \\ y \end{bmatrix}, \quad Q = \begin{bmatrix} F \\ -mg \end{bmatrix}. \quad (38)$$

The constraint equation is $\dot{y} = 0$. Take the derivative to time and write in the form of (6) as $A\ddot{q} = 0$ with $A = [0 \quad 1]$.

No Jacobian matrix is needed as x, y are chosen to be generalized coordinates. According to analysis in Section III & IV, simple symbolic calculation leads to

$$\begin{aligned} F_n = Q_{id}^c &= M^{\frac{1}{2}} \left(AM^{-\frac{1}{2}}\right)^{+} (b - AM^{-1}Q) \\ &= \begin{bmatrix} m^{\frac{1}{2}} & 0 \\ 0 & m^{\frac{1}{2}} \end{bmatrix} \begin{bmatrix} 0 \\ m^{\frac{1}{2}} \end{bmatrix} \left(0 - \begin{bmatrix} 0 & m^{-1} \end{bmatrix} \begin{bmatrix} F \\ -mg \end{bmatrix}\right) \\ &= \begin{bmatrix} 0 \\ mg \end{bmatrix}. \end{aligned} \quad (39)$$

Thus, the friction force $f = [-\mu mg \quad 0]^T$, with the $-$ sign representing the direction.

For the sticking phase, according to (26), the friction force is $-F_t(t)$ when $\dot{q} = 0$ and $\|F_t\| \leq \|F_s\|$. And, according to (20), the tangent force leads to

$$\begin{aligned} F_t(t) &:= (I - A^+A)Q \\ &= (I - \begin{bmatrix} 0 \\ 1 \end{bmatrix}\begin{bmatrix} 0 & 1 \end{bmatrix})\begin{bmatrix} F \\ -mg \end{bmatrix} \\ &= \begin{bmatrix} F \\ 0 \end{bmatrix} \end{aligned} \tag{40}$$

Thus, the friction force $f = [-F \quad 0]^T$ with the sign that represents the direction. This simple case validates somehow intuitively on the effectiveness of the proposed approach.

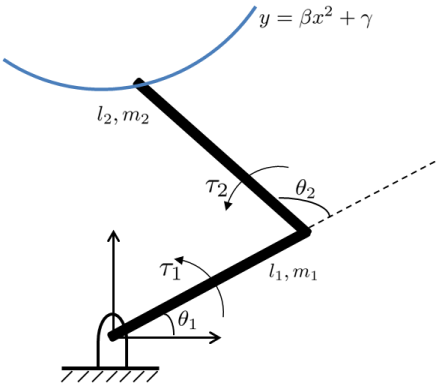

FIGURE 4. Two-link planar manipulator system.

We then go to the nonlinear friction problems. Consider a two-link planar manipulator shown in Figure 4. Assume all masses exist as point masses at the distal end of each link, these masses are m_1 and m_2. Denote θ_1, θ_2 as rotational displacement of the links, we then have the dynamic motion equations of the unconstrained manipulator as [31]:

$$\begin{aligned} \tau_1 &= m_2l_2^2(\ddot{\theta}_1+\ddot{\theta}_2)+m_2l_1l_2\cos\theta_2(2\ddot{\theta}_1+\ddot{\theta}_2)+(m_1 \\ &\quad +m_2)l_1^2\ddot{\theta}_1-m_2l_1l_2\sin\theta_2\dot{\theta}_2^2-2m_2l_1l_2\sin\theta_2\dot{\theta}_1\dot{\theta}_2 \\ &\quad +m_2l_2g\cos(\theta_1+\theta_2)+(m_1+m_2)l_1g\cos\theta_1 \end{aligned} \tag{41}$$

$$\begin{aligned} \tau_2 &= m_2l_1l_2\cos\theta_2\ddot{\theta}_1+m_2l_1l_2\sin\theta_2\dot{\theta}_1^2 \\ &\quad +m_2l_2g\cos(\theta_1+\theta_2)+m_2l_2^2(\ddot{\theta}_1+\ddot{\theta}_2) \end{aligned} \tag{42}$$

The above equations can be written in the matrix form of (1) with

$$q = \begin{bmatrix} \theta_1 \\ \theta_2 \end{bmatrix}, \quad M = \begin{bmatrix} m_{11} & m_{12} \\ m_{12} & m_{22} \end{bmatrix}, \quad Q = \begin{bmatrix} h_1 \\ h_2 \end{bmatrix}, \tag{43}$$

where

$$m_{11} = m_2l_2^2+2m_2l_1l_2\cos\theta_2+(m_1+m_2)l_1^2, \tag{44}$$

$$m_{12} = m_2l_2^2+m_2l_1l_2\cos\theta_2, \tag{45}$$

$$m_{22} = m_2l_2^2, \tag{46}$$

$$\begin{aligned} h_1 &= \tau_1+m_2l_1l_2\sin\theta_2\dot{\theta}_2(\dot{\theta}_2+2\dot{\theta}_1)-m_2l_2g\cos(\theta_1+\theta_2) \\ &\quad -(m_1+m_2)l_1g\cos\theta_1, \end{aligned} \tag{47}$$

$$h_2 = \tau_2-m_2l_1l_2\sin\theta_2\dot{\theta}_1^2-m_2l_2g\cos(\theta_1+\theta_2). \tag{48}$$

Now assume the distal end of link 2 is constrained by a parabola-trajectory governed by $y = \beta x^2+\gamma$. Here x, y is the planar coordinate at the distal end of link 2, β, γ are constants. Assume that the friction force between the distal end of link 2 and the parabola-trajectory is non-negligible. The kinetic friction coefficient is μ and the maximum possible stiction coefficient is μ_s. Note that this is quite a practical problem in which the closed-form of friction force is hard to achieve by any other current known methods due to the normal force is nonconstant.

Since $x = l_1\cos\theta_1+l_2\cos(\theta_1+\theta_2)$, $y = l_1\sin\theta_1+l_2\sin(\theta_1+\theta_2)$ use the generalized coordinates θ_1, θ_2, the constraint will be $l_1\sin\theta_1+l_2\sin(\theta_1+\theta_2)-\beta(l_1\cos\theta_1+l_2\cos(\theta_1+\theta_2))^2-\gamma = 0$. Take time derivative twice, we have the second order form constraint as in (6) with

$$\begin{aligned} A &= \big[2\beta(l_1\cos\theta_1+l_2\cos(\theta_1+\theta_2))(l_2\sin(\theta_1+\theta_2) \\ &\quad +l_1\sin\theta_1)+l_1\cos\theta_1+l_2\cos(\theta_1+\theta_2), \\ &\quad 2\beta(l_1\cos\theta_1+l_2\cos(\theta_1+\theta_2))l_2\sin(\theta_1+\theta_2) \\ &\quad +l_2\cos(\theta_1+\theta_2)\big], \end{aligned} \tag{49}$$

$$\begin{aligned} b &= l_1\sin\theta_1\dot{\theta}_1+l_2\sin(\theta_1+\theta_2)(\dot{\theta}_1+\dot{\theta}_2)^2 \\ &\quad -2\beta(l_1\sin\theta_1\dot{\theta}_1+l_2\sin(\theta_1+\theta_2)(\dot{\theta}_1+\dot{\theta}_2))^2 \\ &\quad -2\beta(l_1\cos\theta_1+l_2\cos(\theta_1+\theta_2))(l_1\cos\theta_1\dot{\theta}_1^2 \\ &\quad +l_2\cos(\theta_1+\theta_2)(\dot{\theta}_1+\dot{\theta}_2)^2). \end{aligned} \tag{50}$$

From expressions of x, y, we have the Jacobian matrix

$$J = \begin{bmatrix} -l_1\sin\theta_1-l_2\sin(\theta_1+\theta_2) & -l_2\sin(\theta_1+\theta_2) \\ l_1\cos\theta_1+l_2\cos(\theta_1+\theta_2) & l_2\cos(\theta_1+\theta_2) \end{bmatrix}. \tag{51}$$

With the M, Q, A, b and J given above, the closed-form expressions of the Coulomb-stiction model can be obtained as in (28), whose closed-form is given in Appendix B. We intendedly list the complex-in-look closed-form representations of friction force for the readers' information, as it might be convincing that the closed-form friction forces in any non-block-simple mechanical systems are rather complex and difficult to achieve by any other current known methods. With the closed-form expressions of Coulomb friction and stiction, the closed-form of the extended friction models can be derived as in Section V.

We do numerical simulation by using the Coulomb-Static friction model for illustration. The Baumgarte's numerical stabilization method [32] is employed to eliminate numerical errors in simulation. For the system parameters, we choose $m_1 = 1$, $m_2 = 1$, $l_1 = 1$, $l_2 = 2$, $g = 9.8$ and $\mu = 0.1$. Assume the manipulator system is constrained by the trajectory governed by $y = 1/4\ x^2$ (i.e. $\beta = 1/4$, $\gamma = 0$), and the system input $\tau_1 = 5\sin t$ is a periodical function of the time t, the input $\tau_2 = 2$ is constant. The system is then doing a reciprocating movement at the distal end of link 2, and the normal force at the contact surface is nonconstant. Figure 5 shows the variety of the norm of the resultant normal force. Since the system is moving in a two dimensional space, we show the movement and the friction force by the two dimensions. Figure 6 (a) shows the reciprocating moving

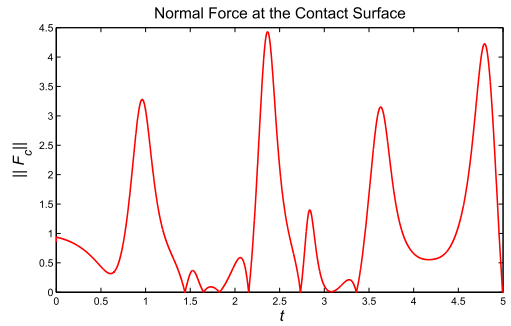

FIGURE 5. The norm of the normal force at the contact surface, it is nonconstant.

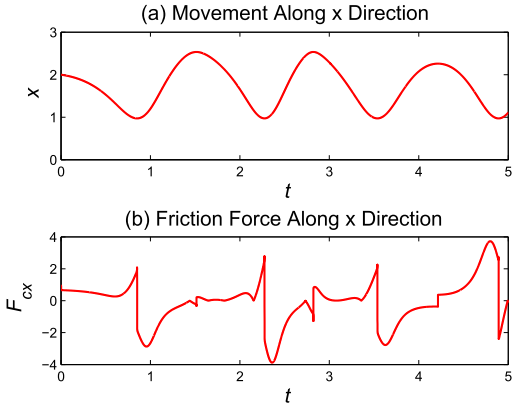

FIGURE 6. Reciprocating movement of the distal end of link 2 along *x* direction and the corresponding Coulomb friction force along *x* direction.

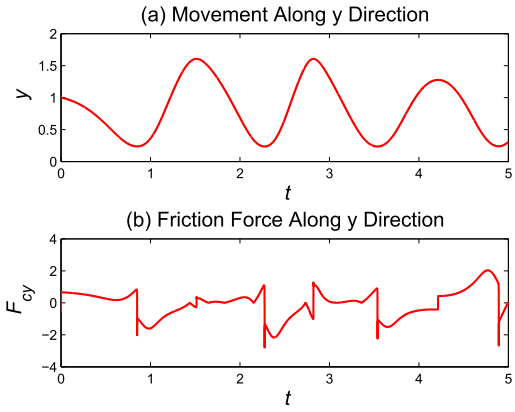

FIGURE 7. Reciprocating movement of the distal end of link 2 along *y* direction and the corresponding Coulomb friction force along *y* direction.

trajectory of the distal end of link 2 along x direction, the corresponding Coulomb friction force along the direction is shown in Figure 6 (b). Similarly, the movement of the distal end of link 2 and the friction force along y direction is shown in Figure 7 (a,b). We see that the closed-form friction force serves the system well and presents certain stick-slip performances. For further comparison information, normal numerical approaches (e.g., Lagrange approach with using Lagrange multipliers) for doing system simulation with friction force can hardly get consistent results with different simulate steps, as they only can employ recursive normal forces, where the cumulative error can hardly be eliminated.

VII. CONCLUSION AND PROSPECTS

By friendly combination with the current known friction models, the literature succeeds to provide the closed-form expressions of friction force in constrained mechanical systems. Closed-form friction models are introduced including the classic Coulomb friction and stiction models, as well as the extended friction models, no matter whether the normal force exerted between the contact surfaces is constant or not. We take the proposed modeling approach as an adequate supplement to current known friction models, which may open a new way for accurate friction force modeling and applications.

Although succeeded in obtaining closed-form expressions of friction force in constrained mechanical systems, there is still much work to do for further research with the help of the proposed closed-form models, e.g., to perform system control design, to model and govern more friction phenomena with nonconstant normal forces and to develop general methods and tools for closed-form modeling of mechanical systems, etc.

APPENDIX A

We cite the mathematical results for reference.

Theorem [30]: Assume Ψ has rank $r \geq 1$, it is true that $\mathcal{R}(\Psi^T) = \mathcal{R}(\Psi^+) = \mathcal{R}(\Psi^+\Psi)$, $\mathcal{N}(\Psi) = \mathcal{R}(I-\Psi^+\Psi)$, where $\mathcal{R}(\cdot)$ and $\mathcal{N}(\cdot)$ denote the range space and null space of the designated matrix, respectively. Then any vector $y \in \boldsymbol{R}^n$ can be decomposed into $\Psi^+\Psi y$, in $\mathcal{R}(\Psi^+)$, and $(I-\Psi^+\Psi)y$, in $\mathcal{R}(I-\Psi^+\Psi)$, i.e., $y = \Psi^+\Psi y+(I-\Psi^+\Psi)y$.

APPENDIX B

The closed-form friction force, represent casewisely, is, when $\dot{q} \neq 0$,

$$
\begin{aligned}
Q_f = \Big[\Big[& -\mu\big((j_1(n_1b_1+n_2b_2)+j_2(n_2b_1+n_3b_2))^2(b-b_3)^2 \\
& +(j_3(n_1b_1+n_2b_2)+j_4(n_2b_1+n_3b_2))^2(b-b_3)^2\big)^{\frac{1}{2}} \\
& \big(((-l_1\sin\theta_1-l_2\sin(\theta_1+\theta_2))\dot{q}_1+(-l_2\sin(\theta_1+\theta_2)) \\
& \dot{q}_2)^2+((l_1\cos\theta_1+l_2\cos(\theta_1+\theta_2))\dot{q}_1+(l_2\cos(\theta_1 \\
& +\theta_2))\dot{q}_2)^2\big)^{-\frac{1}{2}}\big((-l_1\sin\theta_1-l_2\sin(\theta_1+\theta_2)) \\
& ((-l_1\sin\theta_1-l_2\sin(\theta_1+\theta_2))\dot{q}_1+(-l_2\sin(\theta_1+\theta_2))\dot{q}_2) \\
& +(l_1\cos\theta_1+l_2\cos(\theta_1+\theta_2))((l_1\cos\theta_1+l_2\cos(\theta_1 \\
& +\theta_2))\dot{q}_1+(l_2\cos(\theta_1+\theta_2))\dot{q}_2)\big)\Big]; \\
& \Big[-\mu\big((j_1(n_1b_1+n_2b_2)+j_2(n_2b_1+n_3b_2))^2(b-b_3)^2 \\
& +(j_3(n_1b_1+n_2b_2)+j_4(n_2b_1+n_3b_2))^2(b-b_3)^2\big)^{\frac{1}{2}} \\
& \big(((-l_1\sin\theta_1-l_2\sin(\theta_1+\theta_2))\dot{\theta}_1+(-l_2\sin(\theta_1 \\
& +\theta_2))\dot{\theta}_2)^2+((l_1\cos\theta_1-l_2\cos(\theta_1+\theta_2))\dot{\theta}_1+(l_2\cos(\theta_1 \\
& +\theta_2))\dot{\theta}_2)^2\big)^{-\frac{1}{2}}\big((-l_2\sin(\theta_1+\theta_2))((-l_1\sin\theta_1-l_2\sin(\theta_1 \\
& +\theta_2))\dot{\theta}_1+j_2\dot{\theta}_2)+(l_2\cos(\theta_1+\theta_2))((l_1\cos\theta_1-l_2\cos(\theta_1 \\
& +\theta_2))\dot{\theta}_1+(l_2\cos(\theta_1+\theta_2))\dot{\theta}_2)\big)\Big]\Big], \qquad (52)
\end{aligned}
$$

when $\dot{q} = 0$ and $\|F_t\| \leq \|F_s\|$,

$$Q_f = \Big[\Big[-\Big(\big(-l_1\sin\theta_1 - l_2\sin(\theta_1+\theta_2)\big)\big(j_1(1-a_1^2(a_1^2+a_2^2)^{-1})h_1 - a_1a_2h_2(a_1^2+a_2^2)^{-1} + j_2(-a_1a_2h_1(a_1^2+a_2^2)^{-1} + (1-a_2^2(a_1^2+a_2^2)^{-1})h_2)\big) + \big(l_1\cos\theta_1 + l_2\cos(\theta_1+\theta_2)\big)\big(j_3((1-a_1^2(a_1+a_2)^{-1})h_1 - a_1a_2h_2(a_1+a_2)^{-1}) + j_4(-a_1a_2h_1(a_1+a_2)^{-1} + (1-a_2^2(a_1^2+a_2^2)^{-1}))\big)\Big)\Big]; \tag{53}$$

$$\Big[-\Big(-l_2\sin(\theta_1+\theta_2)\big(j_1(1-a_1^2(a_1^2+a_2^2)^{-1})h_1 - a_1a_2h_2(a_1^2+a_2^2)^{-1} + j_2(-a_1a_2h_1(a_1^2+a_2^2)^{-1} + (1-a_2^2(a_1^2+a_2^2)^{-1})h_2)\big) + l_2\cos(\theta_1+\theta_2)\big(j_3((1-a_1^2(a_1+a_2)^{-1})h_1 - a_1a_2h_2(a_1+a_2)^{-1}) + j_4(-a_1a_2h_1(a_1+a_2)^{-1} + (1-a_2^2(a_1^2+a_2^2)^{-1}))\big)\Big)\Big]\Big], \tag{54}$$

and, when $\dot{q} = 0$ and $\|F_t\| > \|F_s\|$,

$$Q_f = \Big[\Big[-\mu_s\Big((j_1(n_1b_1+n_2b_2)+j_2(n_2b_1+n_3b_2))^2(b-b_3)^2 + (j_3(n_1b_1+n_2b_2)+j_4(n_2b_1+n_3b_2))^2(b-b_3)^2\Big)^{\frac{1}{2}}\Big(j_1(1-a_1^2(a_1+a_2)^2h_1 - a_1a_2h_2(a_1^2+a_2^2)^{-1}) + j_2(-a_1a_2h_1(a_1^2+a_2^2)^{-1}) + (1-a_2^2(a_1^2+a_2^2)^{-1})h_2\Big)\Big((j_1(1-a_1^2(a_1+a_2)^2h_1 - a_1a_2h_2(a_1^2+a_2^2)^{-1}) + j_2(-a_1a_2h_1(a_1^2+a_2^2)^{-1}) + (1-a_2^2(a_1^2+a_2^2)^{-1})h_2)^2 + (j_3((1-a_1^2(a_1+a_2)^{-1})h_1 - a_1a_2h_2(a_1+a_2)^{-1}) + j_4(-a_1a_2h_1(a_1+a_2)^{-1} + (1-a_2^2(a_1^2+a_2^2)^{-1})))^2\Big)^{-\frac{1}{2}}\Big];$$

$$\Big[-\mu_s\Big((j_1(n_1b_1+n_2b_2)+j_2(n_2b_1+n_3b_2))^2(b-b_3)^2 + (j_3(n_1b_1+n_2b_2)+j_4(n_2b_1+n_3b_2))^2(b-b_3)^2\Big)^{\frac{1}{2}}\Big(j_3((1-a_1^2(a_1+a_2)^{-1})h_1 - a_1a_2h_2(a_1+a_2)^{-1}) + j_4(-a_1a_2h_1(a_1+a_2)^{-1} + (1-a_2^2(a_1^2+a_2^2)^{-1}))\Big)\Big((j_1(1-a_1^2(a_1+a_2)^2h_1 - a_1a_2h_2(a_1^2+a_2^2)^{-1}) + j_2(-a_1a_2h_1(a_1^2+a_2^2)^{-1}) + (1-a_2^2(a_1^2+a_2^2)^{-1})h_2)^2 + (j_3((1-a_1^2(a_1+a_2)^{-1})h_1 - a_1a_2h_2(a_1+a_2)^{-1}) + j_4(-a_1a_2h_1(a_1+a_2)^{-1} + (1-a_2^2(a_1^2+a_2^2)^{-1})))^2\Big)^{-\frac{1}{2}}\Big]\Big], \tag{55}$$

where,

$$j_1 = \Big(\big((l_1\cos\theta_1 + l_2\cos(\theta_1+\theta_2))^2 + (l_2\cos(\theta_1+\theta_2))^2\big)\big(-l_1\sin\theta_1 - l_2\sin(\theta_1+\theta_2)\big) - \big((-l_1\sin\theta_1 - l_2\sin(\theta_1+\theta_2))(l_1\cos\theta_1 + l_2\cos(\theta_1+\theta_2)) + (-l_2\sin(\theta_1+\theta_2))(l_2\cos(\theta_1+\theta_2))\big)\big(l_1\cos\theta_1 + l_2\cos(\theta_1+\theta_2)\big)\Big)\Big(\big(-l_1\sin\theta_1 - l_2\sin(\theta_1+\theta_2)\big)^2\big(l_2\cos(\theta_1+\theta_2)\big)^2 + \big(-l_2\sin(\theta_1+\theta_2)\big)^2\big(l_1\cos\theta_1 + l_2\cos(\theta_1+\theta_2)\big)^2 - 2\big(-l_1\sin\theta_1 - l_2\sin(\theta_1+\theta_2)\big)\big(l_1\cos\theta_1 + l_2\cos(\theta_1+\theta_2)\big)\big(-l_2\sin(\theta_1+\theta_2)\big)\big(l_2\cos(\theta_1+\theta_2)\big)\Big)^{-1}, \tag{56}$$

$$j_2 = \Big(\big((l_1\cos\theta_1 + l_2\cos(\theta_1+\theta_2))^2 + (l_2\cos(\theta_1+\theta_2))^2\big)\big(-l_2\sin(\theta_1+\theta_2)\big) - \big((-l_1\sin\theta_1 - l_2\sin(\theta_1+\theta_2))(l_1\cos\theta_1 + l_2\cos(\theta_1+\theta_2)) + (-l_2\sin(\theta_1+\theta_2))(l_2\cos(\theta_1+\theta_2))\big)\big(l_2\cos(\theta_1+\theta_2)\big)\Big)\Big(\big(-l_1\sin\theta_1 - l_2\sin(\theta_1+\theta_2)\big)^2\big(l_2\cos(\theta_1+\theta_2)\big)^2 + \big(-l_2\sin(\theta_1+\theta_2)\big)^2\big(l_1\cos\theta_1 + l_2\cos(\theta_1+\theta_2)\big)^2 - 2\big(-l_1\sin\theta_1 - l_2\sin(\theta_1+\theta_2)\big)\big(l_1\cos\theta_1 + l_2\cos(\theta_1+\theta_2)\big)\big(-l_2\sin(\theta_1+\theta_2)\big)\big(l_2\cos(\theta_1+\theta_2)\big)\Big)^{-1}, \tag{57}$$

$$j_3 = \Big(\big((-l_1\sin\theta_1 - l_2\sin(\theta_1+\theta_2))^2 + (-l_1\sin\theta_1 - l_2\sin(\theta_1+\theta_2))^2\big)\big(l_1\cos\theta_1 - l_2\cos(\theta_1+\theta_2)\big) - \big((-l_1\sin\theta_1 - l_2\sin(\theta_1+\theta_2))(l_1\cos\theta_1 + l_2\cos(\theta_1+\theta_2)) + (-l_2\sin(\theta_1+\theta_2))(l_2\cos(\theta_1+\theta_2))\big)\big(-l_1\sin\theta_1 - l_2\sin(\theta_1+\theta_2)\big)\Big)\Big(\big(-l_1\sin\theta_1 - l_2\sin(\theta_1+\theta_2)\big)^2\big(l_2\cos(\theta_1+\theta_2)\big)^2 + \big(-l_2\sin(\theta_1+\theta_2)\big)^2\big(l_1\cos\theta_1 + l_2\cos(\theta_1+\theta_2)\big)^2 - 2\big(-l_1\sin\theta_1 - l_2\sin(\theta_1+\theta_2)\big)\big(l_1\cos\theta_1 + l_2\cos(\theta_1+\theta_2)\big)\big(-l_2\sin(\theta_1+\theta_2)\big)\big(l_2\cos(\theta_1+\theta_2)\big)\Big)^{-1}, \tag{58}$$

$$j_4 = \Big(\big((-l_1\sin\theta_1 - l_2\sin(\theta_1+\theta_2))^2 + (-l_1\sin\theta_1 - l_2\sin(\theta_1+\theta_2))^2\big)\big(l_2\cos(\theta_1+\theta_2)\big) - \big((-l_1\sin\theta_1 - l_2\sin(\theta_1+\theta_2))(l_1\cos\theta_1 + l_2\cos(\theta_1+\theta_2)) + (-l_2\sin(\theta_1+\theta_2))(l_2\cos(\theta_1+\theta_2))\big)\big(-l_2\sin(\theta_1+\theta_2)\big)\Big)\Big(\big(-l_1\sin\theta_1 - l_2\sin(\theta_1+\theta_2)\big)^2\big(l_2\cos(\theta_1+\theta_2)\big)^2 + \big(-l_2\sin(\theta_1+\theta_2)\big)^2\big(l_1\cos\theta_1 + l_2\cos(\theta_1+\theta_2)\big)^2 - 2\big(-l_1\sin\theta_1 - l_2\sin(\theta_1+\theta_2)\big)\big(l_1\cos\theta_1 + l_2\cos(\theta_1+\theta_2)\big)\big(-l_2\sin(\theta_1+\theta_2)\big)\big(l_2\cos(\theta_1+\theta_2)\big)\Big)^{-1}, \tag{59}$$

$$n_1 = \frac{1}{4}(m_{22}^2 - 2m_{22}m_{11} + m_{11}^2 + 4m_{12}^2)^{-\frac{1}{2}}\big(2m_{22} + 2m_{11} - 2(m_{22}^2 - 2m_{22}m_{11} + m_{11}^2 + 4m_{12}^2)^{\frac{1}{2}}\big)^{\frac{1}{2}}$$

$$(m_{22}-2m_{22}m_{11}+m_{11}^2+4m_{12}^2)^{\frac{1}{2}}+m_{11}\big(2m_{22}$$
$$+2m_{11}+2(m_{22}^2-2m_{22}m_{11}+m_{11}^2+4m_{12}^2)^{\frac{1}{2}}\big)^{\frac{1}{2}}$$
$$-m_{11}(2m_{22}+2m_{11}-2(m_{22}^2-2m_{22}m_{11}+m_{11}^2$$
$$+4m_{12}^2)^{\frac{1}{2}})^{\frac{1}{2}}-m_{22}\big(2m_{22}+2m_{11}+2(m_{22}^2$$
$$-2m_{22}m_{11}+m_{11}^2+4m_{12}^2)^{\frac{1}{2}}\big)^{\frac{1}{2}}+m_{22}(2m_{22}+$$
$$2m_{11}-2(m_{22}^2-2m_{22}m_{11}+m_{11}^2+4m_{12}^2)^{\frac{1}{2}}\big)^{\frac{1}{2}}$$
$$+(m_{22}^2-2m_{22}m_{11}+m_{11}^2+4m_{12}^2)^{\frac{1}{2}}\big(2m_{22}+2m_{11}$$
$$+2(m_{22}^2-2m_{22}m_{11}+m_{11}^2+4m_{12}^2)^{\frac{1}{2}}\big), \tag{60}$$

$$n_2 = \frac{1}{2}(m_{22}^2-2m_{22}m_{11}+m_{11}^2+4m_{12}^2)^{-\frac{1}{2}}m_{12}\Big(-\big(2$$
$$m_{22}+2m_{11}+2(m_{22}^2-2m_{22}m_{11}+m_{11}^2+m_{12}^2)^{\frac{1}{2}}\big)$$
$$+\big(2m_{22}+2m_{11}-2(m_{22}^2-2m_{22}m_{11}+m_{11}^2$$
$$+4m_{12}^2)^{\frac{1}{2}}\big)\Big), \tag{61}$$

$$n_3 = \frac{1}{4}(m_{22}^2-2m_{22}m_{11}+m_{11}^2+4m_{12}^2)^{-\frac{1}{2}}\big(2m_{22}$$
$$+2m_{11}-2(m_{22}^2-2m_{22}m_{11}+m_{11}^2+4m_{12}^2)^{\frac{1}{2}}\big)^{\frac{1}{2}}$$
$$(m_{22}-2m_{22}m_{11}+m_{11}^2+4m_{12}^2)^{\frac{1}{2}}+m_{22}\big(2m_{22}$$
$$+2m_{11}+2(m_{22}^2-2m_{22}m_{11}+m_{11}^2+4m_{12}^2)^{\frac{1}{2}}\big)^{\frac{1}{2}}$$
$$-m_{22}\big(2m_{22}+2m_{11}-2(m_{22}^2-2m_{22}m_{11}+m_{11}^2$$
$$+4m_{12}^2)^{\frac{1}{2}}\big)^{\frac{1}{2}}-m_{11}(2m_{22}+2m_{11}+2(m_{22}^2$$
$$-2m_{22}m_{11}+m_{11}^2+4m_{12}^2)^{\frac{1}{2}})^{\frac{1}{2}}+m_{11}\big(2m_{22}+$$
$$2m_{11}-2(m_{22}^2-2m_{22}m_{11}+m_{11}^2+4m_{12}^2)^{\frac{1}{2}}\big)^{\frac{1}{2}}$$
$$+(m_{22}^2-2m_{22}m_{11}+m_{11}^2+4m_{12}^2)^{\frac{1}{2}}\big(2m_{22}+2m_{11}$$
$$+2(m_{22}^2-2m_{22}m_{11}+m_{11}^2+4m_{12}^2)^{\frac{1}{2}}\big), \tag{62}$$

$$b_1 = (a_1n_3-a_2n_2)(n_1n_3-n_2^2)^{-1}\big((a_1n_3-a_2n_2)(n_1n_3$$
$$-n_2^2)^{-2}+(a_2n_1-a_1n_2)(n_1n_3-n_2^2)^{-2}\big)^{-1}, \tag{63}$$

$$b_2 = (a_2n_1-a_1n_2)(n_1n_3-n_2^2)^{-1}\big((a_1n_3-a_2n_2)(n_1n_3$$
$$-n_2^2)^{-2}+(a_2n_1-a_1n_2)(n_1n_3-n_2^2)^{-2}\big)^{-1}, \tag{64}$$

$$b_3 = (-m_{12}^2+m_{22}m_{11})^{-1}(h_1a_1m_{22}-h_1a_2m_{12}$$
$$-h_2a_1m_{12}+h_2a_2m_{11}), \tag{65}$$

REFERENCES

[1] R. Daniel, "Control of machines with friction: Brian armstrong-Hālouvry," *Automatica*, vol. 28, no. 6, pp. 1285–1287, 1992. [Online]. Available: http://www.sciencedirect.com/science/article/pii/000510989290076R

[2] P. Dahl and A. S. F. Model, *Technical Report tor-0158 (3107-18)-1*. El Segundo, CA, USA: The Aerospace Corporation, 1968.

[3] E. Pennestrì, V. Rossi, P. Salvini, and P. P. Valentini, "Review and comparison of dry friction force models," *Nonlinear Dyn.*, vol. 83, no. 4, pp. 1785–1801, Mar. 2016.

[4] Y. Liu, J. Li, Z. Zhang, X. Hu, and W. Zhang, "Experimental comparison of five friction models on the same test-bed of the micro stick-slip motion system," *Mech. Sci.*, vol. 6, no. 1, p. 15, 2015.

[5] L. Simoni, M. Beschi, G. Legnani, and A. Visioli, "Friction modeling with temperature effects for industrial robot manipulators," in *Proc. IEEE/RSJ Int. Conf. Intell. Robots Syst. (IROS)*, Sep. 2015, pp. 3524–3529.

[6] K. Johanastrom and C. Canudas-de-Wit, "Revisiting the LuGre friction model," *IEEE Control Syst.*, vol. 28, no. 6, pp. 101–114, Dec. 2008.

[7] P. Dupont, B. Armstrong, and V. Hayward, "Elasto-plastic friction model: Contact compliance and stiction," in *Proc. Amer. Control Conf.*, Jun. 2000, pp. 1072–1077.

[8] V. Lampaert, J. Swevers, and F. Al-Bender, "Modification of the leuven integrated friction model structure," *IEEE Trans. Autom. Control*, vol. 47, no. 4, pp. 683–687, Apr. 2002.

[9] F. Al-Bender, V. Lampaert, and J. Swevers, "The generalized maxwell-slip model: A novel model for friction simulation and compensation," *IEEE Trans. Autom. Control*, vol. 50, no. 11, pp. 1883–1887, Nov. 2005.

[10] B. Vau and P. D. Larminat, "Dry friction: Modelling and adaptive compensation," in *Proc. 19th Int. Conf. Syst. Theory, Control Comput. (ICSTCC)*, Oct. 2015, pp. 260–265.

[11] M. Indri, S. Trapani, and I. Lazzero, "Development of a general friction identification framework for industrial manipulators," in *Proc. 42nd Annu. Conf. IEEE Ind. Electron. Soc.*, Oct. 2016, pp. 6859–6866.

[12] M. N. Nevmerzhitskiy, A. V. Vara, K. V. Zmeu, and B. S. Notkin, "Technique for friction model identification in an industrial robot joint using KUKA KR10," in *Proc. Int. Multi-Conf. Ind. Eng. Modern Technol. (FarEastCon)*, Oct. 2018, pp. 1–5.

[13] M. Erdmann, "On a representation of friction in configuration space," *Int. J. Robot. Res.*, vol. 13, no. 3, pp. 240–271, Jun. 1994, doi: 10.1177/027836499401300306.

[14] J. Craig, P. Hsu, and S. Sastry, "Adaptive control of mechanical manipulators," in *Proc. IEEE Int. Conf. Robot. Autom.*, Apr. 1986, pp. 190–195.

[15] J. Ohri, L. Dewan, and M. K. Soni, "Fuzzy adaptive dynamic friction compensator for robot," *Int. J. Syst. Appl., Eng. Develop.*, vol. 2, no. 4, pp. 157–161, 2008.

[16] K. A. J. Verbert, R. Tóth, and R. Babuška, "Adaptive friction compensation: A globally stable approach," *IEEE/ASME Trans. Mechatronics*, vol. 21, no. 1, pp. 351–363, Feb. 2016.

[17] J. Yao, W. Deng, and Z. Jiao, "Adaptive control of hydraulic actuators with LuGre model-based friction compensation," *IEEE Trans. Ind. Electron.*, vol. 62, no. 10, pp. 6469–6477, Oct. 2015.

[18] A. Berger, I. Ioslovich, and P.-O. Gutman, "Time optimal trajectory planning with feedforward and friction compensation," in *Proc. Amer. Control Conf. (ACC)*, Jul. 2015, pp. 4143–4148.

[19] B. D. Bui, N. Uchiyama, and S. Sano, "Nonlinear friction modeling and compensation for precision control of a mechanical feed-drive system," *Sensors Mater.*, vol. 27, no. 10, pp. 971–984, 2015.

[20] W. Wei, H. Dourra, and G. G. Zhu, "Adaptive transfer case clutch touchpoint estimation with a modified friction model," *IEEE/ASME Trans. Mechatronics*, vol. 25, no. 4, pp. 2000–2008, Aug. 2020.

[21] N. Ye, J. Song, and G. Ren, "Model-based adaptive command filtering control of an electrohydraulic actuator with input saturation and friction," *IEEE Access*, vol. 8, pp. 48252–48263, 2020.

[22] Y. Li, L. Ding, Z. Zheng, Q. Yang, X. Zhao, and G. Liu, "A multi-mode real-time terrain parameter estimation method for wheeled motion control of mobile robots," *Mech. Syst. Signal Process.*, vol. 104, pp. 758–775, May 2018. [Online]. Available: http://www.sciencedirect.com/science/article/pii/S0888327017306209

[23] L. Zaidi, J. A. Corrales, B. C. Bouzgarrou, Y. Mezouar, and L. Sabourin, "Model-based strategy for grasping 3D deformable objects using a multi-fingered robotic hand," *Robot. Auto. Syst.*, vol. 95, pp. 196–206, Sep. 2017. [Online]. Available: http://www.sciencedirect.com/science/article/pii/S0921889016308089

[24] X. Liu, G. Zuo, J. Zhang, and J. Wang, "Sensorless force estimation of end-effect upper limb rehabilitation robot system with friction compensation," *Int. J. Adv. Robot. Syst.*, vol. 16, no. 4, 2019, Art. no. 1729881419856132, doi: 10.1177/1729881419856132.

[25] E. B. Arisoy, G. Ren, E. Ulu, N. G. Ulu, and S. Musuvathy, "A data-driven approach to predict hand positions for two-hand grasps of industrial objects," in *Proc. 36th Comput. Inf. Eng. Conf.*, vol. 1, Aug. 2016, Art. no. V01AT02A067, doi: 10.1115/DETC2016-60095.

[26] X. Song, H. Liu, K. Althoefer, T. Nanayakkara, and L. D. Seneviratne, "Efficient break-away friction ratio and slip prediction based on haptic surface exploration," *IEEE Trans. Robot.*, vol. 30, no. 1, pp. 203–219, Feb. 2014.

[27] M. Posa, C. Cantu, and R. Tedrake, "A direct method for trajectory optimization of rigid bodies through contact," *Int. J. Robot. Res.*, vol. 33, no. 1, pp. 69–81, Jan. 2014, doi: 10.1177/0278364913506757.

[28] F. E. Udwadia and R. E. Kalaba, *Analytical Dynamics: A New Approach*. Cambridge, U.K.: Cambridge Univ. Press, 2007.
[29] F. E. Udwadia and R. E. Kalaba, "Explicit equations of motion for mechanical systems with nonideal constraints," *J. Appl. Mech.*, vol. 68, no. 3, pp. 462–467, Oct. 2000, doi: 10.1115/1.1364492.
[30] Y.-H. Chen, "Constraint-following servo control design for mechanical systems," *J. Vibrat. Control*, vol. 15, no. 3, pp. 369–389, Mar. 2009, doi: 10.1177/1077546307086895.
[31] J. J. Craig, *Introduction to Robotics: Mechanics Control, 3/E*. London, U.K.: Pearson, 2009.
[32] J. Baumgarte, "Stabilization of constraints and integrals of motion in dynamical systems," *Comput. Methods Appl. Mech. Eng.*, vol. 1, no. 1, pp. 1–16, Jun. 1972. [Online]. Available: http://www.sciencedirect.com/science/article/pii/0045782572900187

JIN HUANG received the B.E. and Ph.D. degrees from the College of Mechanical and Vehicle Engineering, Hunan University, Changsha, China, in 2006 and 2012, respectively.

He was a joint Ph.D. Student with the George W. Woodruff School of Mechanical Engineering, Georgia Institute of Technology, Atlanta, GA, USA, from 2009 to 2011. Since 2013, he has been holding a postdoctoral position with Tsinghua University, Beijing, China, where he has been an Assistant Research Professor, since 2016. His research interests include artificial intelligence in intelligent transportation systems, dynamics control, and fuzzy engineering.

XINGYU LI is currently pursuing the B.S. degree in mechanical engineering with the School of Vehicle and Mobility, Tsinghua University, Beijing, China.

His research interest includes dynamics control.

HUIQIAN LI received the B.S. degree in mechanical engineering from the Beijing Institute of Technology, Beijing, China, in 2020. He is currently pursuing the Ph.D. degree with the School of Vehicle and Mobility, Tsinghua University, Beijing.

His research interests include motion planning and control for autonomous vehicles.

YE-HWA CHEN received the B.S. degree in chemical engineering from National Taiwan University, Taipei, Taiwan, in 1979, and the M.S. and Ph.D. degrees in mechanical engineering from the University of California, Berkeley, CA, USA, in 1983 and 1985, respectively.

He is currently a Professor with the George W. Woodruff School of Mechanical Engineering, Georgia Institute of Technology, Atlanta, GA, USA. His research interests include fuzzy dynamical systems, fuzzy reasoning, and modeling and control of mechanical systems.

ZHIHUA ZHONG received the Ph.D. degree in engineering from Linköping University, Sweden, in 1988.

He is currently a Professor with the School of Vehicle and Mobility, Tsinghua University, Beijing, China. He was an elected Member of the Chinese Academy of Engineering, in 2005. His research interests include auto collision security technology, the punching and shaping technologies of the auto body, modularity and light-weighing auto technologies, and vehicle dynamics.